SIMPLIFIED, PHYSICALLY-INFORMED MODELS OF DISTORTION AND OVERDRIVE GUITAR EFFECTS PEDALS

David T. Yeh, Jonathan S. Abel and Julius O. Smith

Center for Computer Research in Music and Acoustics (CCRMA)
Stanford University, Stanford, CA
[dtyeh|abel|jos]@ccrma.stanford.edu

ABSTRACT

This paper explores a computationally efficient, physically informed approach to design algorithms for emulating guitar distortion circuits. Two iconic effects pedals are studied: the "Distortion" pedal and the "Tube Screamer" or "Overdrive" pedal. The primary distortion mechanism in both pedals is a diode clipper with an embedded low-pass filter, and is shown to follow a nonlinear ordinary differential equation whose solution is computationally expensive for real-time use. In the proposed method, a simplified model, comprising the cascade of a conditioning filter, memoryless nonlinearity and equalization filter, is chosen for its computationally efficient, numerically robust properties. Often, the design of distortion algorithms involves tuning the parameters of this filter-distortion-filter model by ear to match the sound of a prototype circuit. Here, the filter transfer functions and memoryless nonlinearities are derived by analysis of the prototype circuit. Comparisons of the resulting algorithms to actual pedals show good agreement and demonstrate that the efficient algorithms presented reproduce the general character of the modeled pedals.

1. INTRODUCTION

Guitarists tend to feel that digital implementations of distortion effects sound inferior to the original analog gear. This work attempts to provide a more accurate simulation of guitar distortion and a physics based method for designing the algorithm according to the virtual analog approach[1, 2].

Often guitar effects are digitized from a high level understanding of the function of the effect [3, 4]. This work describes the results of a more detailed, physical approach to model guitar distortion. This approach has been adopted previously in the context of generating tube-like guitar distortion [5], not to model a specific effect as done here. This approach starts with the equations that describe the physics of the circuit and is an alternative to obtaining the static transfer curves of a nonlinear system by measurement [6].

Many digital distortion pedals feature pre- and post-distortion filters surrounding a saturating nonlinearity. The filters are commonly multiband (three or four bands) parametric filters that are tuned to taste.

An analysis of the circuits shows that analog solid-state circuits tend to use low-order filters. To keep costs down, circuits are designed with minimal component count, which limits filter order. For the purpose of distortion effect modeling, the frequency range of interest is from just above DC to 20 kHz. Features in the frequency domain above 20 kHz can be ignored, also contributing to low-order filters. Frequency features below 20 Hz must be retained, however, because intermodulation due to mixing of subsonic components with audio frequency components is noticeable in the audio band.

Stages are partitioned at points in the circuit where an active element with low source impedance drives a high impedance load. This approximation is also made with less accuracy where passive components feed into loads with higher impedance. Neglecting the interaction between the stages introduces magnitude error by a scalar factor and neglects higher order terms in the transfer function that are usually small in the audio band.

The nonlinearity may be evaluated as a nonlinear ordinary differential equation (ODE) using numerical techniques [7, 8]. However, the solution of nonlinear ODEs is computationally intensive, and the differences are subtle. Therefore in this work, the nonlinearity is approximated by a static nonlinearity and tabulated. This can be justified on perceptual grounds.

It is well known that nonlinearities cause an expansion of bandwidth that may lead to aliasing if the sampling rate is insufficiently high [3]. Consequently typical digital implementations of distortion upsample by a factor of eight or ten, process the nonlinearities, and downsample back to typical audio rates[3, 9]. Frequency content tends to roll off with increasing frequency, and remaining aliases at oversampling factors of eight or above tend to be masked by the dense spectrum of guitar distortion.

Because the filters in this work are derived from analog prototypes, upsampling also increases the audio band accuracy of the discretization by bilinear transform. An alternate approach would be to design low order filters so that the response at Nyquist matches the continuous time transfer function [10, 11].

The following is an analysis of the stages in two typical distortion pedals.

2. FUNDAMENTAL TOOLS

2.1. SPICE simulation

For circuits that are difficult to analyze, SPICE simulation provides detailed numerical analysis. DC analysis in SPICE performs static sweeps of voltage or current sources to measure memoryless transfer curves. AC analysis finds the frequency response of a circuit linearized about an operating point. These responses can be imported into Matlab and converted to digital filters as in [1]. SPICE also serves as a reference solver for numerical solutions of the time domain response for nonlinear ODEs.

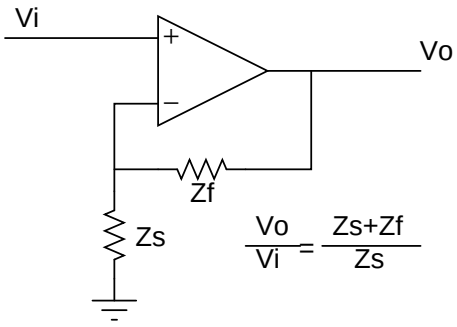

Figure 1: *Non-inverting op amp gain*

2.2. Continuous time pole-zero analysis

Linear circuits are described by rational transfer functions. For most low-cost audio circuits such as guitar effects, the transfer functions are typically low order. The poles and zeros can be identified on a log-frequency plot of magnitude in dB. In dB, it can be seen that the magnitude contributions of poles subtract and the magnitude contributions of zeros add. For the low pass filter, at the pole frequency, the magnitude is 3 dB lower than at its low frequency asymptote. For the high pass filter, the magnitude at the pole frequency is 3 dB lower that at its high frequency asymptote. Therefore, well separated pole and zero frequencies can be identified from the decibel magnitude response by looking for the 3-dB points. These frequencies can then be used to reconstruct the rational expression for the transfer function.

2.3. Analysis of operational amplifier circuits

Transfer functions can be easily found analytically for circuits with operational amplifiers (op amps).

2.3.1. Ideal op amp approximation

The ideal op amp approximation states that if negative feedback is present,

1. $V_+ = V_-$,
2. $I_+ = I_- = 0$

where V_+ is the voltage at the $+$ terminal of the op amp and V_-, the voltage at the $-$ terminal. I_+ and I_- are the currents flowing into the two terminals. These conditions do not hold if negative feedback is not present, for example, if V_o is not connected to V_- or if the op amp output is close to the supply voltages, causing it to clip.

2.3.2. Non-inverting configuration

An example of this analysis is done for the non-inverting op amp configuration shown in Fig. 1. The ideal op amp rule gives $V_- = V_i$, so the current through Z_s is $I_s = V_i/Z_s$. Because $I_- = 0$, all the current flows across Z_f, so $V_0 = V_i + I_s Z_f = V_i + V_i/Z_s$. After algebraic manipulation, the transfer function is found to be $\frac{V_o}{V_i} = \frac{Z_s+Z_f}{Z_s}$. This results in a continuous time transfer function if complex impedances are used for Z_f and Z_s. Writing it in the form shown in (1) allows the poles and zeros to be seen more easily:

$$A_v(s) = \frac{Z_f}{Z_s}\left(\frac{Z_s}{Z_f} + 1\right) \tag{1}$$

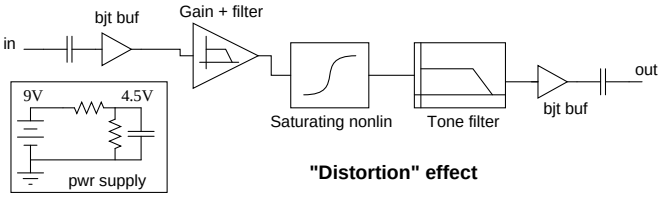

Figure 2: *Block diagram of Distortion pedal.*

2.4. Bilinear Transform of low order transfer functions

Once a continuous time transfer function is obtained either by analysis or by inspection of the magnitude response, the bilinear transform can be used to digitize this filter. First- and second-order continuous time systems are common, so their mappings are given below.

The continuous time system,

$$H(s) = \frac{b_n s^n + ... + b_1 s + b_0}{a_n s^n + ... + a_1 s + a_0}, \tag{2}$$

results in

$$H(z) = \frac{B_0 + B_1 z^{-1} + ... + B_n z^{-n}}{A_0 + A_1 z^{-1} + ... + A_n z^{-n}}, \tag{3}$$

where for a second order system, coefficients of $H(z)$ are

$$B_0 = b_0 + b_1 c + b_2 c^2, \tag{4}$$
$$B_1 = 2b_0 - 2b_2 c^2, \tag{5}$$
$$B_2 = b_0 - b_1 c + b_2 c^2, \tag{6}$$
$$A_0 = a_0 + a_1 c + a_2 c^2, \tag{7}$$
$$A_1 = 2a_0 - 2a_2 c^2, \tag{8}$$
$$A_2 = a_0 - a_1 c + a_2 c^2, \tag{9}$$

and for a first-order system, coefficients of $H(z)$ are

$$B_0 = b_0 + b_1 c, \tag{10}$$
$$B_1 = b_0 - b_1 c, \tag{11}$$
$$A_0 = a_0 + a_1 c, \tag{12}$$
$$A_1 = a_0 - a_1 c. \tag{13}$$
$$\tag{14}$$

Here $c = 2/T$ is chosen as typical for the bilinear transform.

3. CIRCUIT ANALYSIS OF DISTORTION PEDAL

The block diagram of the Boss DS-1 Distortion pedal [12] is shown in Fig. 2. It is basically gain with a saturating nonlinearity sandwiched between filters. However, distortion from the bipolar transistor (BJT) emitter follower buffers and first gain stage are not negligible.

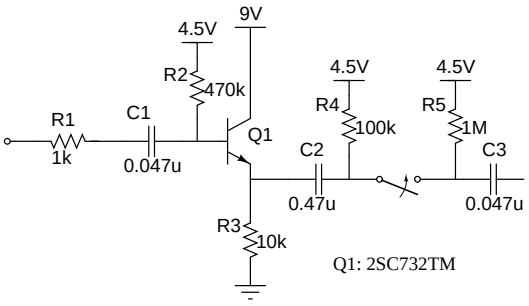

Figure 3: *Input buffer: Emitter follower circuit.*

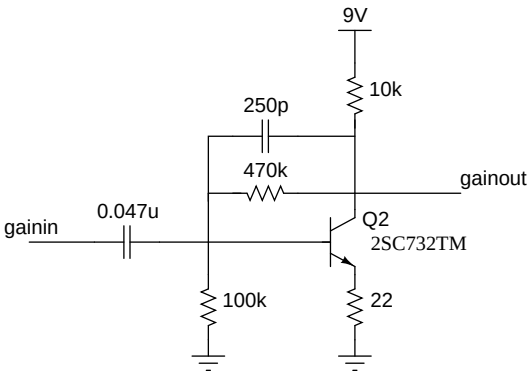

Figure 4: *BJT transimpedance gain*

3.1. Emitter Follower buffers

A typical guitar pedal has an emitter follower (Fig. 3) at the input to buffer the signal from the guitar pickups, and another similar emitter follower at the output to drive the cable and subsequent load. The emitter follower topology is nominally linear in operation and flat in frequency response in the audio band. Typically it is used in conjunction with high pass filters, whose cutoff frequency can be determined from the resistance and capacitance values. Here it is 3 Hz. The stage can be implemented as cascaded low order high pass filters . Implementation of high pass filters is straightforward with the bilinear transform method of digitizing an analog prototype as described in Section 2.

3.2. Single bipolar transistor transimpedance gain stage

Gain can be provided by a single bipolar junction transistor (BJT) in a transimpedance gain topology shown in Fig. 4.

The frequency response is found from SPICE and digitized by finding the continuous time poles and zeros, forming the transfer function and taking the bilinear transform. This stage shows 36 dB of bandpass gain (Fig. 5). There are two zeros at DC, one pole at 3 Hz, one pole at 600 Hz, and another at 72 kHz, which is ignored because it is well outside the audio band. A transfer function is formed directly in (15):

$$H(s) = \frac{s^2}{(s+\omega_1)(s+\omega_2)}, \tag{15}$$

where the numerator is the product of two zeros, s, and the denominator is the product of the poles at $\omega_1 = 2\pi 3$ and $\omega_1 = 2\pi 600$.

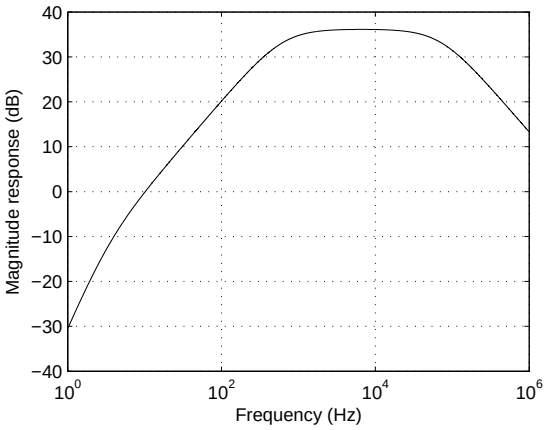

Figure 5: *Frequency response of BJT stage*

The bilinear transform applied to $H(s)$ with a sampling rate $f_s = 44.1$ kHz gives a second order digital filter whose coefficients can be found using (9).

This stage introduces significant nonlinearity at large inputs, but this is neglected for now.

3.3. Op amp gain stage

Non-inverting op amp "buffers" are common in guitar circuits because they minimize loading on the preceding stage. To analyze the circuit in Fig. 6 impedances are used in (1). The final transfer function in factored form is given by (16).

$$H(s) = \frac{(s+\frac{1}{R_t C_c})(s+\frac{1}{R_b C_z}) + \frac{s}{R_b C_c}}{(s+\frac{1}{R_t C_c})(s+\frac{1}{R_b C_z})} \tag{16}$$

where $R_t = D{\cdot}100\text{k}\Omega$, $R_b = (1-D)100\text{k}\Omega{+}4.7\text{k}\Omega$, $C_z = 1\mu$F, and $C_c = 250$pF. Capacitor C_z blocks DC to prevent the output from saturating in the presence of DC offset, while C_c stabilizes the op amp and contributes a low pass pole. D ranges between $(0, 1)$ and is the value of the "DIST" knob that controls the amount of gain before saturation and therefore the intensity of the distortion.

The frequency response is shown in Fig. 7 for values of D from 0 to 1 in increments of 0.1. This is a second-order stage than can be digitized directly by the bilinear transform, forming a second-order section with variable coefficients. The frequency response of this stage depends on the "DIST" knob. Notice that the frequency response at half the audio sampling rate, $|H(f = 22050)|$, is not zero and considerable warping will take place without oversampling or the filter design method by Orfanidis [10].

This transfer function can be discretized by the bilinear transform, (9), which also preserves the mapping of the "DIST" parameter.

The op amp provides the main nonlinearity of the Distortion effect. To first order, the op amp hard clips the signal at $V_{dd}/2$. In reality the op amp response is much slower because it is open loop and needs to recover from overdrive. It is also typically asymmetrical in behavior, leading to significant even-order harmonics where otherwise only odd-order harmonics are expected. Refinements of the op amp clipping model can be based upon the macromodeling technique as done in SPICE to speed up simulations [13]. A

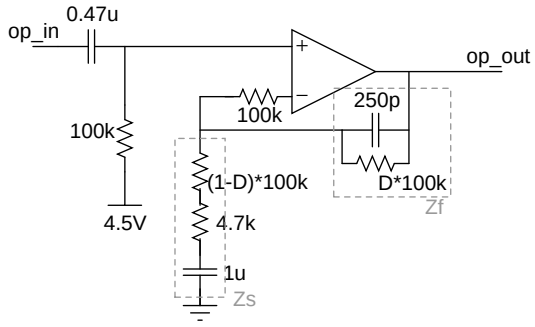

Figure 6: *Operational amplifier gain stage*

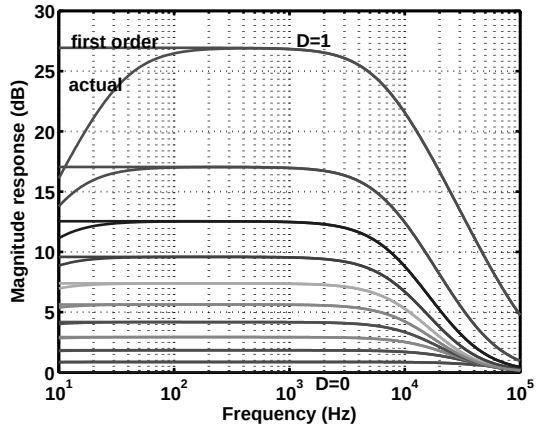

Figure 7: *Frequency response of op amp gain stage,* $D = 0 : 0.1 : 1$

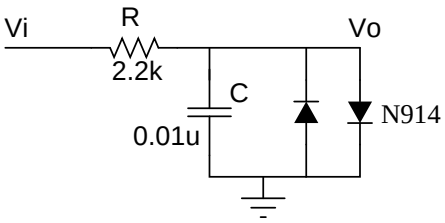

Figure 8: *RC low pass filter with diode limiter*

black box approach, the macromodeling technique emulates the input/output behavior of the op amp instead of simulating the behavior of its internal devices.

3.4. Diode clipper

Following the op amp clipper is a RC low pass filter with a diode limiter across the capacitor (Fig. 8). The diode clipper limits the voltage excursion across the capacitor to about a diode drop in either direction about signal ground.

The model of the pn diode is

$$I_d = I_s(e^{V/V_t} - 1), \tag{17}$$

where the reverse saturation current I_s, and thermal voltage V_t of

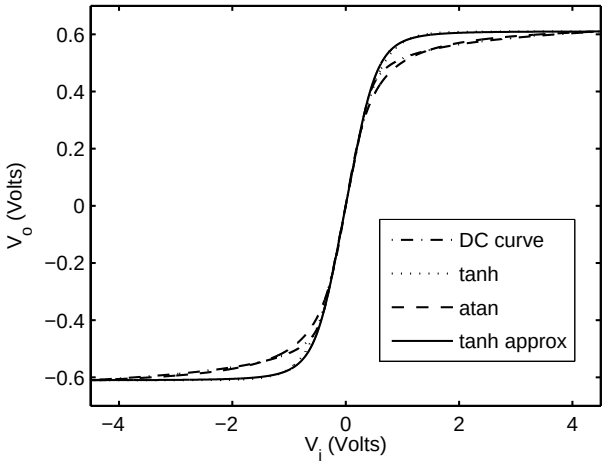

Figure 9: *Static nonlinear functions compared: tabulated, tanh, arctan, approximation to tanh*

the device are model parameters that can be extracted from measurement.

The nonlinear ODE of the diode can be derived from Kirchhoff's laws:

$$\frac{\mathrm{d}V_o}{\mathrm{d}t} = \frac{V_i - V_o}{RC} - 2\frac{I_s}{C}(\sinh(V_o/V_t)), \tag{18}$$

where V_i, V_o are the input and output signals respectively.

This is not a memoryless nonlinearity because it is a low-pass filter whose pole location changes with voltage. Fig. 10 depicts the input-output characteristic, which can be described as a "clipping" function, along with various analytic approximations based on hyperbolic tangent and arctangent. At high amplitude levels, the differences between different clipping functions is subtle.

For efficiency, this nonlinearity is approximated as static, and the DC transfer curve is computed by setting $\frac{\mathrm{d}V_o}{\mathrm{d}t} = 0$ in (18), and tabulating the function $V_o = f(V_i)$ by Newton iteration. A nonuniform sampling of the input to output transfer curve is used that utilizes a constant error percentage or signal to quantization noise ratio. The rationale for this is that at small amplitudes, the curve is most linear with the highest gain, and most susceptible to quantization noise. At high levels, the nonlinearity is compressive, reducing the gain and quantization error. A logarithmic sampling with a floor about zero is chosen. Linear interpolation is used to further reduce quantization noise.

Alternatively an approximation such as

$$\frac{x}{(1 + |x|^n)^{1/n}} \tag{19}$$

can be used to compute the nonlinearity. This formula (19) well approximates hyperbolic tangent when $n = 2.5$. The transfer curve of the tabulated function is compared with that of tanh, arctan, and (19) in Fig. 9. The curves are normalized so that the slope about $V_i = 0$ matches visually and V_o at the extremes match. The formula (19) can be seen to be a good approximation of tanh. Arctan looks like a close approximation to the actual DC nonlinearity but it is not as linear about $V_i = 0$. The approximation (19) has the advantage of an additional parameter n that can be varied to better

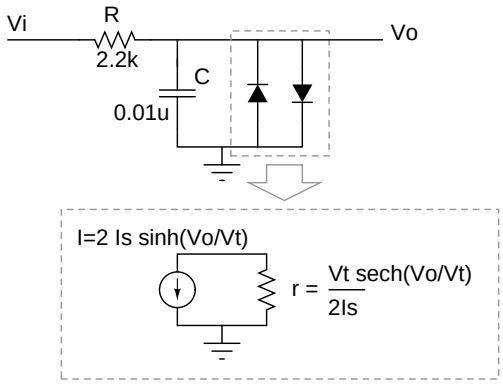

Figure 10: *Small signal approximation of diode clipper*

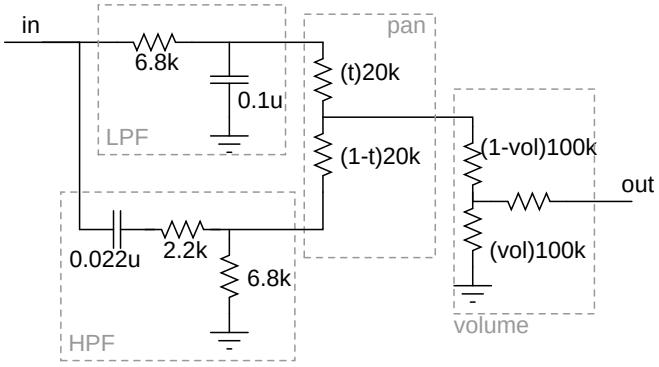

Figure 11: *Tone circuit of Distortion pedal*

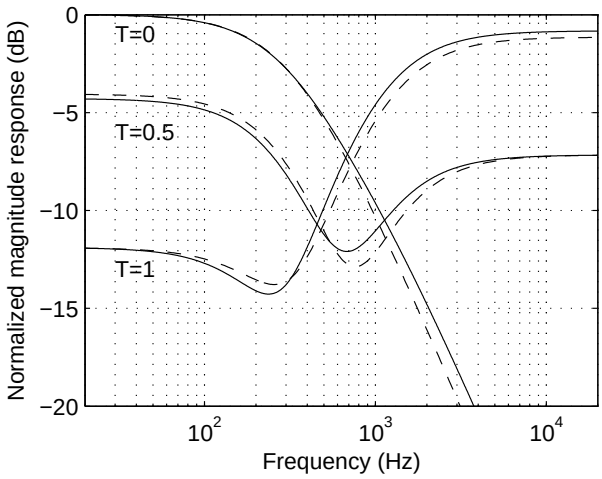

Figure 12: *Distortion pedal tone circuit frequency response. Solid line is actual. Dashed line is digitized implementation.*

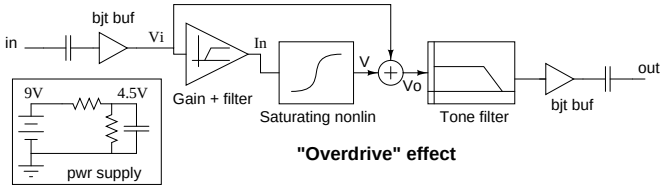

Figure 13: *Block diagram of Overdrive pedal.*

match the actual function. In this work, the tabulated nonlinearity is chosen.

3.5. Tone stage

The tone stage (Fig. 11) is a highly interconnected passive network that cannot be accurately separated. However, an analysis of the circuit shows its design intent, and the error due to separating the blocks is less than that due to component tolerance in an actual circuit.

This circuit involves a fade between high pass filter and low pass filter blocks. The fading affects the cutoff frequencies of the filters, but this effect is small. A digitization of this circuit can capture the essence of its operation, which is a loudness boost: a V-shaped equalization as commonly observed for tone circuits intended for electric guitars[5, 1].

A full analysis is straightforward but tedious, so AC analysis is performed in SPICE, and the corner frequencies found graphically. The weightings for the fade are also determined by simulation. The high pass corner frequency is $f_{hpf} = 1.16$ kHz and the low pass corner frequency is $f_{lpf} = 320$ Hz.

This is implemented digitally as a weighted sum of first-order high pass and low pass filters discretized by the bilinear transform rather than discretizing the complete transfer function. This simplification eliminates time-varying filters and the computation to update the coefficients, using static coefficients instead. Modeling a user controlled parameter with greater accuracy is unnecessary because a user would not likely notice the difference in filter response.

The magnitude response of the original circuit is compared with the Matlab approximation in Fig. 12. The responses are very similar with < 1 dB error in most cases.

4. CIRCUIT ANALYSIS OF OVERDRIVE PEDAL

The block diagram of an overdrive pedal, specifically the Ibanez Tube Screamer, is given in Fig. 13[14]. It is characterized by high pass filters, followed by the summation of a high-pass filtered and clipped signal summed with the input signal. This is followed by low-pass tone filtering and a high pass in the output buffer. The following is an analysis of the circuit in rigor

4.1. High pass filters

The first stages of the overdrive pedal are high pass filters with the following cutoff frequencies: $f_{c1} = 15.9$ Hz, $f_{c2} = 15.6$ Hz.

4.2. Non-inverting op amp with diode limiter

The non-inverting op amp (Fig. 14) of the overdrive pedal is similar to that of the distortion except the diode limiter is now across Z_f. The diode limiter essentially limits voltage excursion across the op amp keeping it within ideal op amp conditions. The voltage at the minus input of the op amp is then the same as that on the

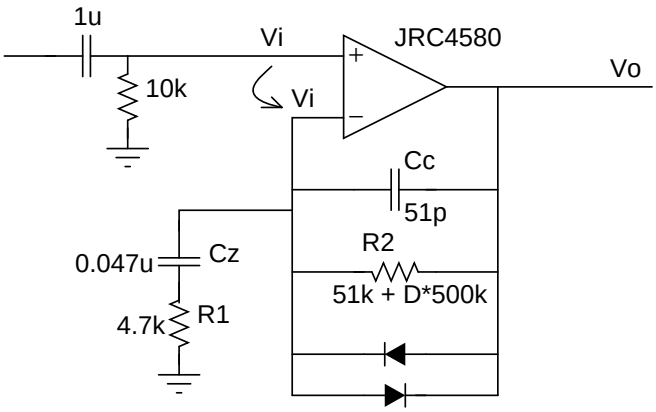

Figure 14: *Clipping stage of overdrive pedal.*

plus terminal. This generates a current across Z_s,

$$I_n = \frac{V_{neg}}{Z_s} = V_i \frac{s}{R_1(s+\omega_z)}, \tag{20}$$

where $\omega_z = (R_1 C_z)^{-1}$, $R_1 = 4.7\text{k}\Omega$, $C_z = 0.047\mu$F. I_n flows through the components connected between the minus terminal and the output of the op amp. Circuit analysis produces the following equation:

$$I_n = \frac{V_o - V_i}{R_2} + C_c \frac{\mathrm{d}}{\mathrm{d}t}(V_o - V_i) + 2I_s \sinh(\frac{V_o - V_i}{V_t}) \tag{21}$$

Making a variable substitution $V = V_o - V_i$ yields,

$$\frac{\mathrm{d}V}{\mathrm{d}t} = \frac{I_n}{C_c} - \frac{V}{R_2 C_c} - \frac{2I_s}{C_c} \sinh(V/V_t), \tag{22}$$

where $C_C = 51$pF, $R_2 = 51\text{k} + D500\text{k}$, and $D \in (0, 1)$, controlling the intensity of the overdrive. It can be seen that this ODE is the same as that for the Distortion pedal, (18), when I_n is replaced by V_i/R.

The arithmetic introduced by the variable substitution can be described in block diagram form as depicted in Fig. 13. The essence of the overdrive circuit is the summation of the input signal with the input filtered and clipped. The above variable substitution is solved for V_o:

$$V_o = V + V_i, \tag{23}$$

where V is obtained by solving (22).

4.3. Tone stage

The tone stage (Fig. 15) can also be analyzed according to ideal op amp rules. The algebra is complicated, but the result is

$$\frac{V_o}{V_i} = \frac{(R_l R_f + Y)}{Y R_s C_s} \frac{s + W\omega_z}{(s+\omega_p)(s+\omega_z) + Xs}, \tag{24}$$

where

$$W = \frac{Y}{R_l R_f + Y},$$
$$X = \frac{R_r}{R_l + R_r} \frac{1}{(R_z + R_l \| R_r) C_z},$$
$$Y = (R_l + R_r)(R_z + R_l \| R_r),$$

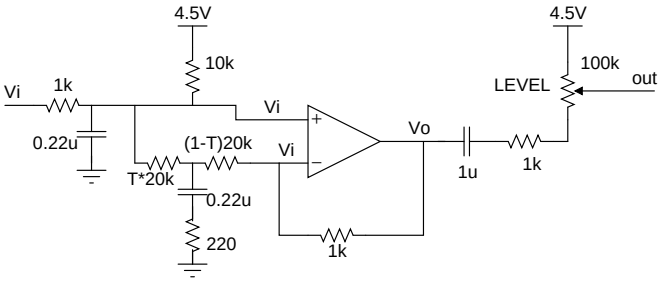

Figure 15: *Overdrive tone circuit.*

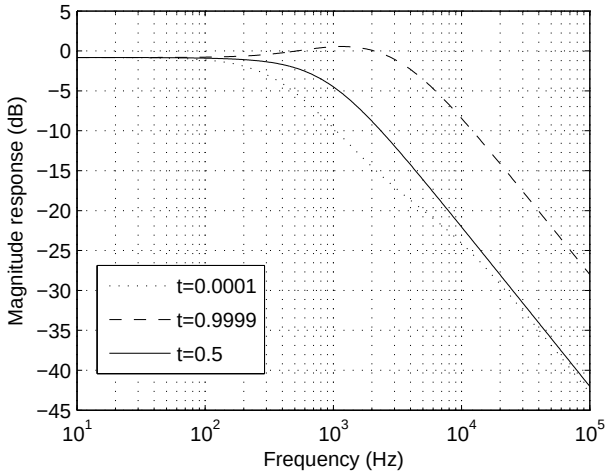

Figure 16: *Overdrive tone circuit frequency response for T = 0, 0.5, 1.*

$\omega_z = 1/(C_z(R_z + R_l \| R_r))$, $\omega_p = 1/(C_s(R_s \| R_i))$, $R_f = 1\text{k}$, $R_r = (1-T)20\text{k}$, $R_l = T20\text{k}$, $R_z = 220$, $C_z = 0.22\mu$F, $R_i = 10\text{k}$, $R_s = 1\text{k}$, $C_s = 0.22\mu$F, and $T \in (0, 1)$ controls the cutoff frequency of the low pass.

This is a second-order transfer function with variable coefficients. Fig. 16 shows the essentially low-pass character of the magnitude response.

5. RESULTS

Actual Distortion and Overdrive pedals are compared to the digital emulations for a 220 Hz sine signal with amplitude of 100 mV, and an exponential sine sweep. The settings on the actual pedal are adjusted until the spectrum resembles that of the digital version for the sine input. Adjustments were made approximately to match the difference in magnitude of the first two harmonics, and to match the position of notches in the frequency domain.

The time waveforms and magnitude spectra for the single-frequency excitation are shown in Figs. 17–20. The sinusoidal sweeps are represented by a log-frequency spectrogram [15] in Figs. 21–24 with 80-dB dynamic range.

The waveforms show a general similarity. The spectrograms indicate that frequency equalization is close. The measured spectra exhibit a strong even-order nonlinearity that is not modeled in the digital implementation. The emulated versions using the simplified algorithms in both cases sound slightly brighter than the

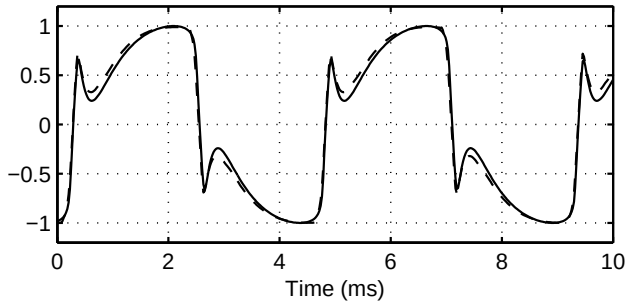

Figure 17: *Time response to 220 Hz sine, measured distortion pedal (dashed) and algorithm (solid)*

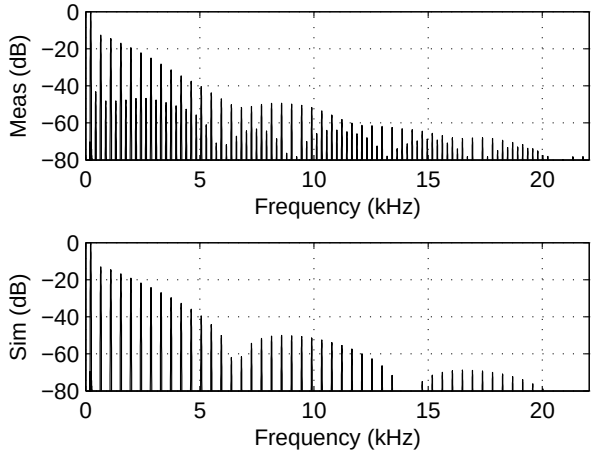

Figure 18: *Normalized spectrum of response to 220 Hz sine, distortion pedal (top), algorithm (bottom)*

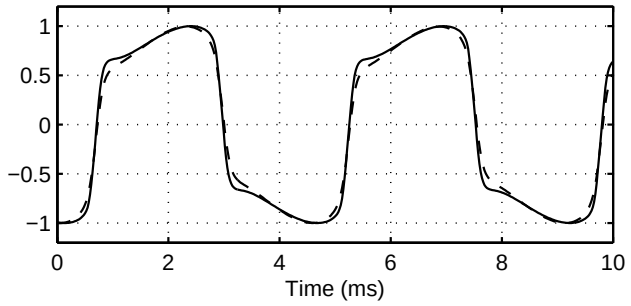

Figure 19: *Time response to 220 Hz sine, measured overdrive pedal (dashed) and algorithm (solid)*

actual pedals, possibly due to the lack of even-order nonlinearity and a difference in equalization..

The digitally emulated result also deviates from the measured one because there was no attempt to calibrate the model to the actual pedal with its particular component values and parameter settings. It is more representative of a circuit whose components are exactly the values as in the schematic.

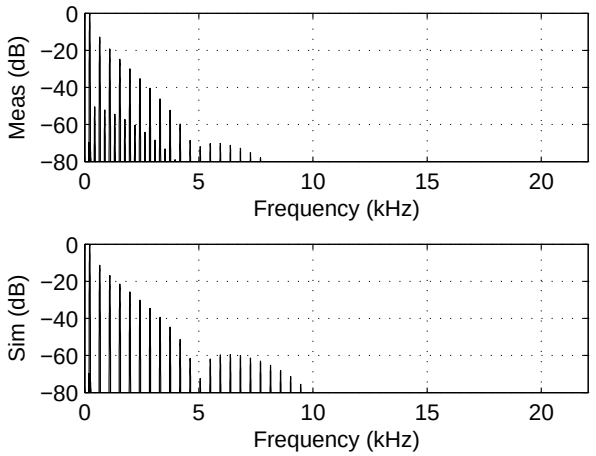

Figure 20: *Normalized spectrum of response to 220 Hz sine, overdrive pedal (top), algorithm (bottom)*

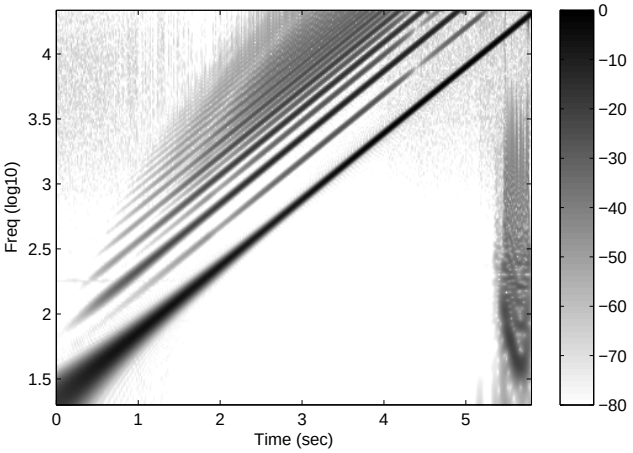

Figure 21: *Measured distortion pedal, sine sweep log spectrogram*

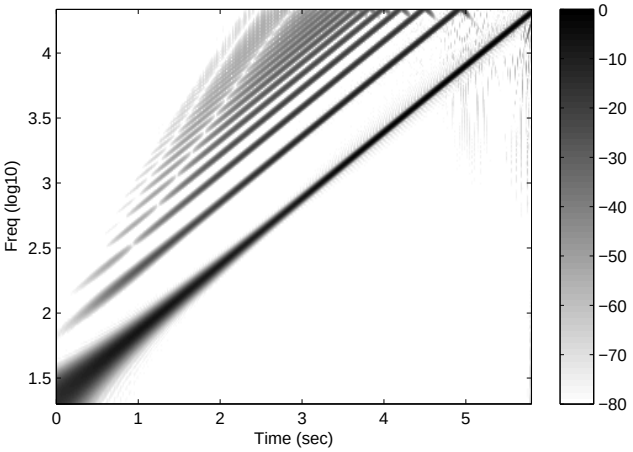

Figure 22: *Distortion algorithm, sine sweep log spectrogram*

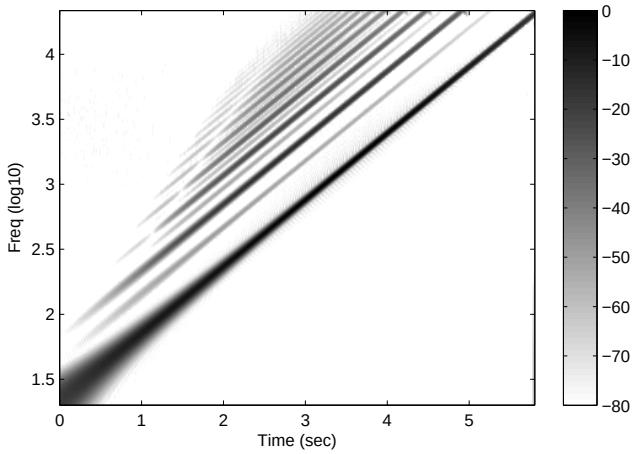

Figure 23: *Measured overdrive pedal, sine sweep log spectrogram*

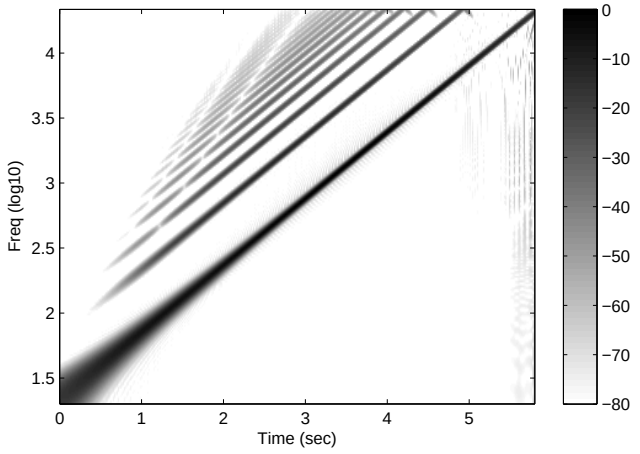

Figure 24: *Overdrive algorithm, sine sweep log spectrogram*

6. CONCLUSIONS

The simplified, physically informed approach enables the design of distortion algorithms that emulate the behavior of analog prototypes. A first-pass design with no tuning is able to reproduce the salient characteristics of the effect.

While the result is not an exact emulation of the analog implementation, it provides a procedural basis for the design of a distortion algorithm, and a starting point from which further tuning can be done. The computational power needed is comparable to that available in commercially available guitar effects boxes because of the similar architecture comprising oversampling, low order filters, and a tabulated nonlinearity.

In this work, BJT gain stage and op amp clipping behaviors are oversimplified. Nonlinearities are assumed to come from a single symmetrical diode clipper, which is not true under large-signal conditions. Improved models of remaining nonlinearities are the subject of ongoing research.

7. ACKNOWLEDGMENTS

This work has been supported by the NSF and NDSEG graduate fellowships. Thanks to Digidesign for their critique and insightful comments. Thanks to Boss and Ibanez for producing these unique music processing circuits and their impact on the guitar playing world.

8. REFERENCES

[1] D. T. Yeh and J. O. Smith, "Discretization of the '59 Fender Bassman tone stack," in *Proc. of the Int. Conf. on Digital Audio Effects (DAFx-06)*, Montreal, Quebec, Canada, Sept. 18–20, 2006, pp. 1–6.

[2] A. Huovilainen, "Nonlinear Digital Implementation of the Moog Ladder Filter," in *Proc. of the Int. Conf. on Digital Audio Effects (DAFx-04)*, Naples, Italy, Oct. 5–8, 2004.

[3] U. Zölzer, Ed., *DAFX - Digital Audio Effects*, J. Wiley & Sons, 2002.

[4] J. Schimmel, "Using nonlinear amplifier simulation in dynamic range controllers," in *Proc. of the Int. Conf. on Digital Audio Effects (DAFx-03)*, London, UK, Sep. 8-11 2003.

[5] M. Karjalainen, T. Mäki-Patola, A. Kanerva, and A. Huovilainen, "Virtual air guitar," *Journal of the AES*, vol. 54, no. 10, pp. 964–980, Oct. 2006.

[6] S. Möller, M. Gromowski, and U. Zölzer, "A measurement technique for highly nonlinear transfer functions," in *Proc. of the Int. Conf. on Digital Audio Effects (DAFx-02)*, Hamburg, Germany, Sep. 26-28 2002, pp. 203–206.

[7] M. Karjalainen and J. Pakarinen, "Wave digital simulation of a vacuum-tube amplifier," in *IEEE ICASSP 2006 Proc.*, Toulouse, France, 2006, vol. 5, pp. 153–156.

[8] D. T. Yeh, J. Abel, and J. O. Smith, "Simulation of the diode limiter in guitar distortion circuits by numerical solution of ordinary differential equations," in *Proc. of the Int. Conf. on Digital Audio Effects (DAFx-07)*, Bordeaux, France, Sept. 10–15, 2007.

[9] M. Doidic and et al., "Tube modeling programmable digital guitar amplification system," U.S. Patent 5789689, Aug. 16 1998.

[10] S. J. Orfanidis, "Digital parametric equalizer design with prescribed nyquist-frequency gain," *Journal of the AES*, vol. 45, no. 6, pp. 444–455, June 1997.

[11] D. P. Berners and J. S. Abel, "Discrete-time shelf filter design for analog modeling," in *Proc. 115th AES Convention*, New York, Oct. 2003.

[12] Roland Corp., *Boss DS-1 Service Notes*, Dec. 26 1980.

[13] G. R. Boyle, D. O. Pederson, B. M. Cohn, and J. E. Solomon, "Macromodeling of integrated circuit operational amplifiers," *IEEE J. Solid-State Circuits*, vol. 9, pp. 353–364, Dec 1974.

[14] R. G. Keen, "The Technology of the Tube Screamer," Available at http://www.geofex.com/fxtech.htm, Accessed Mar 22, 2007.

[15] J. C. Brown, "Calculation of a constant Q spectral transform," *J. Acoust. Soc. Am*, vol. 89, pp. 425–434, 1991, Matlab code available at http://web.media.mit.edu/ brown/cqtrans.htm.